Inorganic Chemistry

Article

pubs.acs.org/IC

Theoretical Studies on Polynuclear $\{Cu^{II}_5Gd^{III}_n\}$ Clusters (n = 4, 2): Towards Understanding Their Large Magnetocaloric Effect

Thayalan Rajeshkumar,[†] Harshini V. Annadata,[†] Marco Evangelisti,[§] Stuart K. Langley,[‡] Nicholas F. Chilton,[‡,⊥] Keith S. Murray,[‡] and Gopalan Rajaraman*[,†]

[†]Department of Chemistry, Indian Institute of Technology Bombay, Powai, Mumabi 400076, India

[§]Instituto de Ciencia de Materiales de Aragón and Departamento de Física de la Materia Condensada, CSIC-Universidad de Zaragoza, 50009 Zaragoza, Spain

[‡]School of Chemistry, Monash University, Clayton, Victoria 3800, Australia

[⊥]School of Chemistry, The University of Manchester, Manchester M13 9PL, United Kingdom

Supporting Information

ABSTRACT: Density functional theory (DFT) studies on two polynuclear clusters, $[Cu^{II}_5Gd^{III}_4O_2(OMe)_4(teaH)_4(O_2CC(CH_3)_3)_2(NO_3)_4]$ (**1**) and $[Cu_5Gd_2(OH)_4(Br)_2(H_2L)_2(H_3L)_2(NO_3)_2(OH_2)_4]$ (**2**), have been carried out to probe the origin of the large magnetocaloric effect (MCE). The magnetic exchange interactions for **1** and **2** via multiple pathways are estimated using DFT calculations. While the calculated exchange parameters deviate from previous experimental estimates obtained by fitting the magnetic data, the DFT parameter set is found to offer a striking match to the magnetic data for both complexes, highlighting the problem of over-parameterization. Magnetostructural correlations for {Cu−Gd} pairs have been developed where both the Cu−O−Gd angles and Cu−O−Gd−O dihedral angles are found to significantly influence the magnitude and sign of the exchange constants. The magnitude of the MCE has been examined as a function of the exchange interactions, and clues on how the effect can be enhanced are discussed.

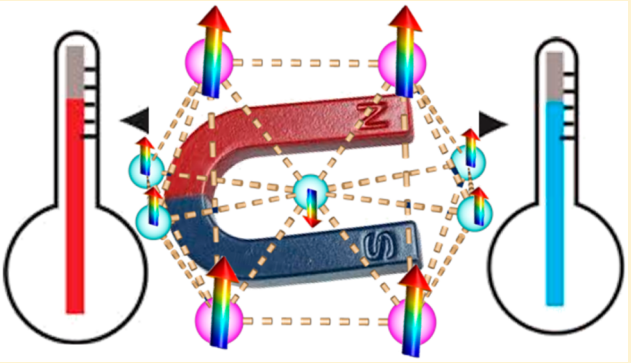

INTRODUCTION

Magnetic refrigeration is a potential application, based on the magnetocaloric effect (MCE), that has aroused great interest recently.[1] In the magnetic refrigeration cycle, a change in the magnetic entropy (ΔS_m) of the refrigerant upon removing the magnetic field (under adiabatic conditions) leads to the cooling of the system, forming the basis of the MCE. The MCE was first discovered by Weiss and Piccard,[2] but the explanation of the process in paramagnetic salts and its potential use in cooling applications were given later by Debye and Giauque.[3,4] The use of the MCE for cooling has recently been proposed as a replacement for the highly expensive helium-3.[5]

All paramagnetic substances exhibit the MCE, but certain polynuclear clusters containing paramagnetic ions, often termed as molecular nano magnets (MNMs),[6−8] have been found to possess large ΔS_m values. The study of the MCE in magnetic molecules began with the first generation of MNMs, compounds based on 3d metals such as $\{Fe_8\}$ and $\{Mn_{12}\}$, and reached a pinnacle with the largest MCE found in an $\{Fe_{14}\}$ cluster with an S = 25 ground state.[9,10] More recently, significant impetus gathered in the field after the discovery of a large MCE in lanthanide based MNMs, particularly for several {3d-Gd}[11−24] and {Gd−Gd}[25−31] complexes. In order to observe a large MCE, the complex of interest should possess a large spin ground state, which should be isotropic in nature. The gain in magnetic entropy is significantly higher if the effective ground state of the molecular complex is degenerate in nature which can be visualized by $S_m = nR\ln(2S + 1)$ (where S_m = magnetic entropy, n = degeneracy, R = gas constant, S = effective ground spin state). Often excited states of the complexes can also contribute to the magnetic entropy; thus the superexchange interaction between the metal centers should be negligible in order to exploit the degree of freedom provided by these excited state levels to the magnetic entropy. Gd(III)-containing complexes are thus ideal candidates to obtain large MCE values as they satisfy all the prerequisites outlined above. It is therefore generally found that Gd(III) based complexes[11−31] display the best performing cooling properties for magnetic based coolants, with the record[32] change in entropy observed for a gadolinium-metal organic framework (MOF), i.e., $Gd(HCOO)_3$, with a ΔS_m value of −55.9 J kg^{-1} K^{-1} for an applied field change of ΔB = 7 T.[33]

Received: November 3, 2014
Published: January 23, 2015

DOI: 10.1021/ic502651w
Inorg. Chem. 2015, 54, 1661−1670

Although numerous examples of molecular species possessing large $-\Delta S_m$ values have now been reported, the search for molecules with a large MCE continues to be of interest to the community. Over recent years, theoretical methods have become a powerful tool to understand and predict properties of several MNMs.[11,34−44] Recently, some of us have undertaken detailed theoretical studies on several {3d-Gd}[11,39−41] and {Gd−Gd}[38,43] complexes to compute the magnetic exchange and to underpin the mechanism of magnetic coupling in this class of molecule. Since the magnetic exchange can be correlated to the $-\Delta S_m$ values, theoretical methods can therefore be utilized to rationalize the observed MCE, and they can also offer viable ways to fine-tune the properties. Although Gd(III) ions are ideal building blocks for clusters designed for a large MCE, many homometallic Gd(III) dinuclear and polynuclear complexes are reported to possess antiferromagnetic coupling.[27,45,46] This often results in a diamagnetic ground state at lower temperatures which is not ideal for cooling applications. On the other hand, heterometallic {3d-Gd} complexes enjoy the advantage of often displaying ferromagnetic coupling where, for example, magnetically isotropic 3d ions such as Cu(II) have gained much attention, and several {Cu−Gd} clusters have been reported in the literature with notable MCE values (see Table 1).[12,16,18,19,30,34,44,47,48] To gain insight into the Cu···Gd exchange interaction in polynuclear complexes and to understand how the magnetic exchange therein contributes to $-\Delta S_m$, we have chosen to study two structurally related {Cu−Gd} complexes. The first, a $[Cu^{II}_5Gd^{III}_4]$ (**1**) compound reported by Murray et al.,[12] possesses one of the highest entropy change ($-\Delta S_m$) for its class ($\Delta S_m = -31$ J kg^{-1} K^{-1} at $T = 3$ K for $\Delta B_0 = 9$ T), and the second, a $[Cu^{II}_5Gd^{III}_2]$ (**2**) cluster reported by Powell et al.,[49] has a very similar structural motif to that in complex **1**. Employing density functional theory (DFT), we have computed the magnetic exchange interactions in complexes **1** and **2** and have explored the correlation with the observed $-\Delta S_m$ values. Attempts have been made to develop correlation between $-\Delta S_m$ values and the Cu···Gd J values.

Table 1. $-\Delta S_m$ Values for Selected 3d-4f Complexes

complexes	ΔH (kOe)	$-\Delta S_m$ (J kg^{-1} K^{-1})
$\{Mn_3Gd_2\}_n$[17]	70	50.1
$\{Co_{10}Gd_{42}\}$[16]	70	41.3
$\{Ni_{12}Gd_{36}\}$[20]	70	36.3
$\{Cu_{36}Gd_{24}\}$[47]	70	35.7
$\{Cu_3Gd_6\}$[19]	70	34.5
$\{Mn_4Gd_6\}$[21]	70	33.7
$\{Co_4Gd_{10}\}$[22]	70	32.6
$\{Cu_5Gd_4\}$[12]	90	31.0
$\{Cr_2Gd_3\}$[23]	90	28.7
$\{Co_6Gd_8\}$[24]	70	28.6
$\{Mn_9Gd_9\}$[21]	70	28.0
$\{Ni_6Gd_6\}$[14]	70	26.5
$\{Cu_2Gd_2\}_n$[44]	70	25.7

COMPUTATIONAL DETAILS

The metal ions in **1** and **2** are labeled as shown in Figure 1. To evaluate the exchange interactions between the different metal centers in **1**, the following exchange Hamiltonian has been employed,

$$\begin{aligned}\hat{H}_{Ex} = -[&2J_1(\hat{S}_{Cu3}\hat{S}_{Cu4} + \hat{S}_{Cu3}\hat{S}_{Cu5} + \hat{S}_{Cu3}\hat{S}_{Cu6} + \hat{S}_{Cu3}\hat{S}_{Cu7}) \\ &+ 2J_2(\hat{S}_{Cu4}\hat{S}_{Cu5} + \hat{S}_{Cu6}\hat{S}_{Cu7}) + 2J_3(\hat{S}_{Cu3}\hat{S}_{Gd1} + \hat{S}_{Cu3}\hat{S}_{Gd2} \\ &+ \hat{S}_{Cu3}\hat{S}_{Gd8} + \hat{S}_{Cu3}\hat{S}_{Gd9}) + 2J_4(\hat{S}_{Cu6}\hat{S}_{Gd1} + \hat{S}_{Cu4}\hat{S}_{Gd2} + \hat{S}_{Cu4}\hat{S}_{Gd9} \\ &+ \hat{S}_{Cu6}\hat{S}_{Gd8} + \hat{S}_{Cu7}\hat{S}_{Gd1} + \hat{S}_{Cu5}\hat{S}_{Gd2} + \hat{S}_{Cu7}\hat{S}_{Gd8} + \hat{S}_{Cu5}\hat{S}_{Gd9}) \\ &+ 2J_5(\hat{S}_{Gd1}\hat{S}_{Gd2} + \hat{S}_{Gd8}\hat{S}_{Gd9}) + 2J_6(\hat{S}_{Gd1}\hat{S}_{Gd8} + \hat{S}_{Gd2}\hat{S}_{Gd9})] \end{aligned} \quad (1)$$

Here J is the isotropic exchange coupling constant, with S_{Gd} and S_{Cu} representing the spins of gadolinium and copper ions. In the case of **2**, we employed a similar Hamiltonian except for the J_6 interaction which was not required.

$$\begin{aligned}\hat{H}_{Ex} = -[&2J_1(\hat{S}_{Cu3}\hat{S}_{Cu4} + \hat{S}_{Cu3}\hat{S}_{Cu5} + \hat{S}_{Cu3}\hat{S}_{Cu6} + \hat{S}_{Cu3}\hat{S}_{Cu7}) \\ &+ 2J_2(\hat{S}_{Cu4}\hat{S}_{Cu5} + \hat{S}_{Cu6}\hat{S}_{Cu7}) + 2J_3(\hat{S}_{Cu3}\hat{S}_{Gd1} + \hat{S}_{Cu3}\hat{S}_{Gd2}) \\ &+ 2J_4(\hat{S}_{Cu6}\hat{S}_{Gd2} + \hat{S}_{Cu7}\hat{S}_{Gd2} + \hat{S}_{Cu5}\hat{S}_{Gd1} + \hat{S}_{Cu4}\hat{S}_{Gd1}) \\ &+ 2J_5^*(\hat{S}_{Gd1}\hat{S}_{Gd2}) \end{aligned} \quad (2)$$

The energies of eight spin configurations for **1** and seven spin configurations for **2** are computed to extract the exchange interaction and also to compute the error bars in the estimated J values (see Supporting Information for details).[50] The computed spin configurations for **1** and **2** are given in the Supporting Information as Tables ST11 and ST12. From the energies of these spin configurations and expressing them by a pairwise interaction model, the exchange coupling constants have been estimated using the broken symmetry (BS) approach developed by Noodleman.[51] This method has previously been employed to compute reasonable estimates of exchange interactions in numerous polynuclear complexes including several {3d-4f} systems.[11,41,52,53] In accordance with our earlier method assessment for a {Cu−Gd} pair,[54] we have employed the B3LYP[55] functional in conjunction with a TZV[56] basis set for all atoms except for Gd, where the relativistically corrected ECP basis set of Cundari−Steven[57] (CSDZ) was employed. All the calculations are performed with the Gaussian 09 suite of programs.[58] The magnetic properties were simulated using the MAGPACK software[59] and the $-\Delta S_m$ calculations have been computed using PHI.[60]

RESULTS AND DISCUSSION

Complex **1** $[Cu^{II}_5Gd^{III}_4O_2(OMe)_4(teaH)_4(O_2CC(CH_3)_3)_2(NO_3)_4]$ is a nonanuclear cluster consisting of five Cu(II) and four Gd(III) ions (Figure 1a). Experimental magnetic measurements suggest an $S = {}^{31}/_2$ ground state which can be visualized as spin down on the central copper ion and spin up on all the other ions. The heat capacity measurements revealed a very large MCE of $-\Delta S_m \approx 31$ J kg^{-1} K^{-1} at 3 K and $\Delta B = 9$ T.[12] This is one of the largest $-\Delta S_m$ values reported for a {3d-4f} cluster to date.[61] Further magnetic analysis undertaken on this complex by fitting a featureless $\chi_M T$ curve predicted a $S = {}^{23}/_2$ ground state.[62] Since multiple J's were employed to fit a featureless curve, there could be multiple solutions which can fit the data, and thus the obtained ground spin-state was realized to be ambiguous. Exchange coupling constants (J) obtained from the best fit of the magnetic data to Hamiltonian eq 1 are shown in Table 2 and labeled J_{exp}. Complex **2** $[Cu_5Gd_2(OH)_4(Br)_2(H_2L)_2(H_3L)_2(NO_3)_2(OH_2)_4]$, on the other hand, comprises five Cu(II) ions and two Gd(III) ions (Figure 1b). The structure of **2** is strikingly similar to complex **1**, where the difference is an absence of two Gd(III) ions from **1**. Magnetic studies reveal an $S = {}^{17}/_2$ ground state which can be obtained using a spin down configuration on the central Cu(II) ions and spin-up on other ions (see Table 2).[49]

DOI: 10.1021/ic502651w
Inorg. Chem. 2015, 54, 1661−1670

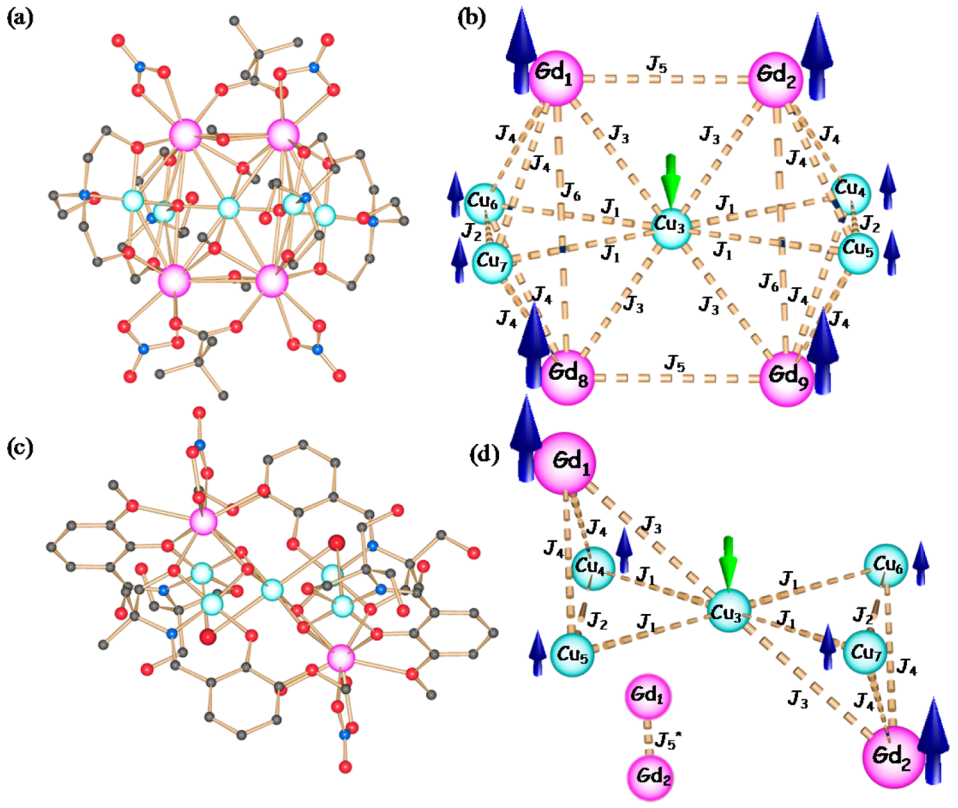

Figure 1. (a) Molecular structure of **1**; (b) exchange pathways in **1**; (c) molecular structure of **2**; (d) exchange pathways in **2**.

Table 2. DFT and Experimental Exchange Coupling Constants (J Values) for 1 and 2

	J_{exp} (cm^{-1})		J_{DFT} (cm^{-1})			
			full cluster		simple dinuclear models	
magnetic exchange parameters	**1**	**2**	**1**	**2**	**1**	**2**
J_1 (Cu···Cu)	0.10	~ −69.3	−91.50	−14.80	−118.56	−14.36
J_2 (Cu···Cu)	−0.16	~ −69.3	−20.19	−4.10	−20.39	−2.59
J_3 (Cu···Gd)	−0.02	~0.69	−1.08	1.68	−0.29	
J_4 (Cu···Gd)	−0.09	~0.69	0.34	2.17	1.24	
J_5 (Gd···Gd)	0.11		−0.07	−0.06		
J_6 (Gd···Gd)			0.13			

The exchange topology employed for the calculations are shown in Figure 1b for **1** and Figure 1d for **2**. DFT and experimentally determined J values are very different for both complexes (Table 2). However, simulation of the magnetic properties with the computed exchange constants reproduces the magnetic data for both **1** and **2** (see Figure 2a–d). In addition to this the $-\Delta S_m$ data collected for complex **1** is also reproduced using the computed J values (vide infra). A minor deviation in the low temperatures $\chi_M T$ data is observed for **1**, and a slight perturbation on the Gd–Gd exchange (see below) yields a perfect fit to the experimental data (see Supporting Information, Figure SF8). This highlights the complexity involved in extracting the magnetic exchange in large polynuclear clusters, and, in the next section, we discuss the individual exchange pathways and probe their origins using DFT.

Exchange Coupling Analysis. *Cu···Cu Interactions.* In complex **1**, both J_1 and J_2 describe the Cu···Cu interactions. Calculations on the full structure yielded a J_1 value of −91.5 cm^{-1} for compound **1**. This is in contrast to the Cu···Cu exchange values obtained from the experimental susceptibility fit using MAGPACK where a weak ferromagnetic coupling (0.1 cm^{-1}) was suggested. To confirm the validity of the computed results, we calculated this interaction using the diamagnetic substitution method[58] and dinuclear model complex (see Table 2 and SD1 for further discussion). The above calculations confirm the strong antiferromagnetic nature of the J_1 interaction with difference in their magnitude compared to the full structure calculations. The magnetic exchange in dinuclear Cu(II) compounds has been shown to be strongly correlated to the Cu–O–Cu angle[64−66] where more obtuse angles yield antiferromagnetic interactions and more acute angles yield ferromagnetic interactions. The Cu–O–Cu angles involved in the J_1 pathway are 129.0 and 123.9 deg. These angles are much larger than the threshold value of 93.6 deg and would therefore be expected to yield strong antiferromagnetic exchange pathways, assuming the simple model holds. As these angles are quite wide this stimulates a strong interaction between the two $d_{x^2-y^2}$ orbitals of each Cu(II) center[66] and is reflected in the computed overlap integrals (see Supporting Information, Figure SF1 for magnetic orbitals and spin density

DOI: 10.1021/ic502651w
Inorg. Chem. 2015, 54, 1661−1670

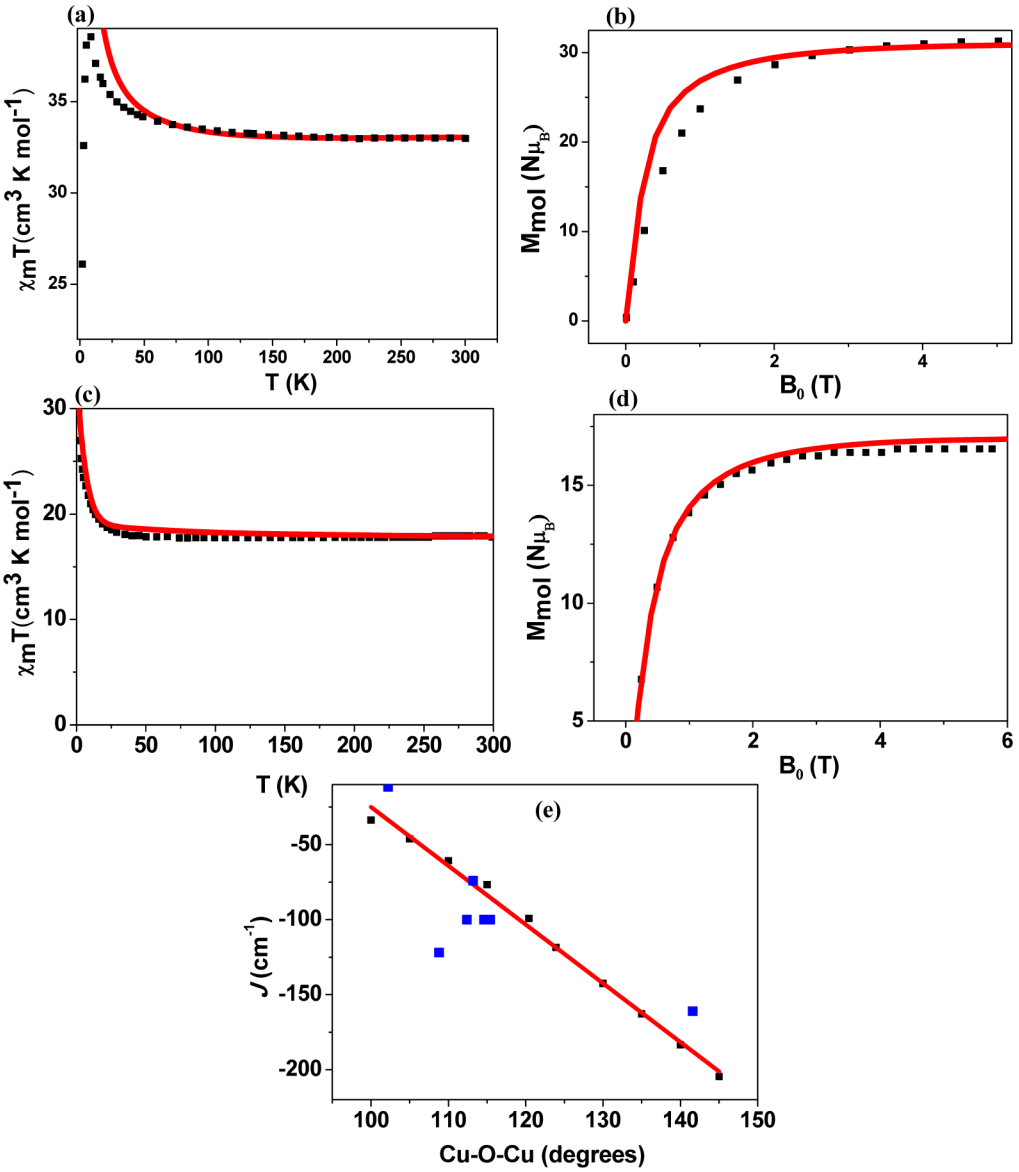

Figure 2. (a) Simulated $\chi_m T$ versus T curve using the calculated DFT J values (red line) and experimental data (black squares) for complex **1**; (b) simulated M versus H curve using the calculated DFT J values (red line) and experimental data (black squares) for complex **1**; (c) simulated $\chi_m T$ versus T curve using the calculated DFT J values (red line) and experimental data (black squares) for complex **2**; (d) simulated M versus H curve using the calculated DFT J values (red line) and experimental data (black squares) for complex **2**; (e) angle correlation developed by varying Cu−O(H)−Cu in a model dimer, best fitting obtained with $y = ax + b$ where $a = -3.916$; $b = 366.66$ (Here black and blue squares represents DFT and experimental J values, respectively.) The isotropic $g = 2.0$ value was used to simulate the above curves.

plot of the computed dinuclear model and SD2 for overlap integral values).

Although numerous correlations have been developed for doubly bridged $\{Cu(OH)_2Cu\}$ cores,[66−68] correlations for single μ-oxo bridged copper dimers have not been reported. To rationalize the computed J values, we have developed a magnetostructural correlation for such a pair by varying the Cu−O(H)−Cu angle in a dinuclear model (see Figure SF2a, Supporting Information) from 100° to 145° (see Figure 2e). A linear dependence for J with the Cu−O(H)−Cu angle was observed, similar to the experimental and theoretical correlations developed for the $\{Cu(OH)_2Cu\}$ pair.[66,67] Experimental examples of such single μ-oxo bridged copper dimers (and trimers)[67,69−71] are superimposed on the correlation diagram, showing a good agreement with the calculated trend and also supporting the strong antiferromagnetic J_1 value for this cluster.

The J_2 interaction in complex **1** is mediated via the central μ_5-oxo bridge as well as an μ_2-alcoholic bridge which is loosely bound to both the Cu(II) centers (see Figure 1b). The J_2 interaction is computed to be −20.19 cm^{-1} when the full cluster is modeled. A drastic reduction for J_2 compared to J_1 is due to the more acute Cu−O(H)−Cu angles (107° for the μ_5-oxo and 73.8° for the OH bridge), and this can be rationalized based on the correlations developed above. The computed J_2 interaction for the model dimer of −20.39 cm^{-1} is found to have close match with full cluster calculations of −20.19 cm^{-1} (see Figure SF2 for structure of model dimers).

The J_1 interaction in complex **2** is mediated via a μ_3-OH group and a μ-Br group. Although the Cu−O(H)−Cu angle is relatively large (113.59−115.31 deg) (see Table ST7 of

DOI: 10.1021/ic502651w
Inorg. Chem. 2015, 54, 1661−1670

Supporting Information) and thus expected to yield a strong antiferromagnetic exchange, the Cu−Br−Cu angle is extremely acute (66.9 deg) and is likely to promote a ferromagnetic contribution to the exchange.[71] This leads overall to a moderately antiferromagnetic interaction, calculated as −14.8 cm^{-1} in the full cluster model. For the dinuclear model, a value of −14.36 cm^{-1} was computed and shows a close resemblance with the J_1 value obtained from the full cluster calculations (see Figure SF3, Supporting Information for structure of model dimers). Moreover, the hydrogen atom of the μ_3-OH group is found to be shifted out of the Cu−O−Cu plane due to a strong H-bonding interaction. This shift is estimated to be 57 deg and can also significantly reduce the J values as shown previously[68] (see SD3 for details for effect of this parameter on the exchange). The J_2 interaction in complex **2** is mediated exclusively via μ-Br groups. Large Cu−Br−Cu angles and long Cu−Br distances (see Supporting Information Table ST8) yield weak antiferromagnetic exchange, resulting in a value of −4.10 cm^{-1} (dinuclear model J = −2.59 cm^{-1}) for this pair.[71] We note here that the large descrepancy between experimental and theoretical J_1 and J_2 interactions is attributed to the fact that experimentally multiple exchange coupling constants were employed to fit featureless $\chi_M T$ data, leading to a case of overparameterization.

Cu···Gd Interactions. J_3 and J_4 denote magnetic interactions between Cu(II) and Gd(III) pairs in both **1** and **2**. Detailed theoretical studies on {$Cu(OR)_2Gd$} complexes have recently been undertaken by us where a mechanism for the magnetic exchange between Cu···Gd pairs was proposed.[54,73] Since earlier studies on correlations for {CuGd} pairs ignores the pivotal role of the Cu−O−Gd angle, we have decided to develop a magnetostructural correlation where both the Cu−O−Gd angles (93.45−102.2 deg) and the Cu−O−Gd-O dihedral angles (0−24.35 deg) are explored simultaneously; see Figure 3. As is evident from the plot, a large dihedral angle

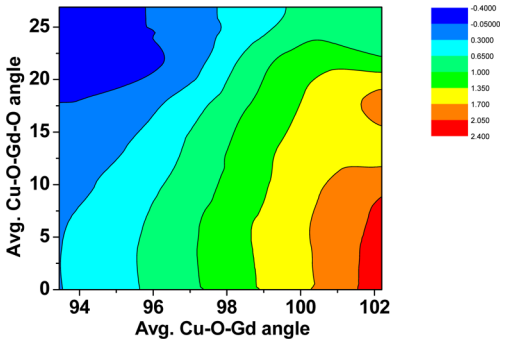

Figure 3. Magnetostructural correlation developed by varying Cu−O−Gd and Cu−O−Gd−O (dihedral) angles simultaneously.

and acute Cu−O−Gd angles lead to antiferromagnetic Cu···Gd interactions, while ferromagnetic couplings are obtained when the Cu−O−Gd angles are large and the Cu−O−Gd-O dihedral angle is small.

Although the Cu−O−Gd−O dihedral angle has been suggested as a key parameter that controls the strength of the magnetic exchange,[54,73] the Cu−O−Gd angle has also been shown to play a major role in determining the nature of the magnetic exchange.[54] The J_3 interaction in complex **1** is mediated via a μ_5-O and two μ_3-O(Me) groups with Cu−O−Gd angles ranging between 83.0 and 96.1°, while the Cu−O−Gd−O dihedral angles are found to range from 25° to 64.1°. Since this interaction has three μ-O bridges[41] with acute Cu−O−Gd angles and larger dihedral angles, this results in antiferromagnetic coupling as can be evidenced from the developed magnetostructural correlations and by the earlier correlation reported by us (see Figure SF4 of Supporting Information).[54]

In complex **1**, the J_4 pathway shows Cu−O−Gd−O dihedral angles in the range 1.5−7.6°, while the Cu−O−Gd angles are found to be in the range 89.0−106.4°. The combination of both small dihedral angles and larger Cu−O−Gd angles favor ferromagnetic coupling,[54] and this leads to a small but ferromagnetic J_4 interaction (see also Figure SF4 and Table ST4, Supporting Information for full list of structural parameters). Calculations performed on model complexes (see Figure SF2 for structure of model dimers) involving J_3 and J_4 pathways correctly reproduce the sign of the magnetic exchange as in the full cluster calculations. Significant overlap between the $d_{x^2-y^2}$ orbital of Cu(II) and 4f orbitals of Gd(III) are detected for the J_3 pathway, while the overlap integrals for the J_4 pathway are found to be drastically reduced. Since a direct 3d-4f overlap contributes to the antiferromagnetic part of the exchange, the overlap integral rationalizes the computed magnetic coupling (see Table ST13 and ST14 of Supporting Information).

For complex **2** the J_3 and J_4 interactions are mediated via μ_3-O(H) and a μ-O(Ph) group, respectively. Here the Cu−O−Gd−O dihedral angles are found to be small (0.8−7.6°) and the Cu−O−Gd angles are found to be in the range of 101.5−106.4°. Such values are associated with ferromagnetic exchange coupling as establisher earlier[54] and in the present correlation, see Figure 3. These structural characteristics are therefore responsible for the calculated exchange parameters of −0.29 and 1.24 cm^{-1}, for J_3 and J_4, respectively.

Gd···Gd Interactions. In complex **1**, the J_5 interaction is mediated through two μ-O(Me) groups and one carboxylate bridge. The magnetic exchange between two Gd(III) ions has been previously established by us to be dependent on the Gd−O−Gd angle.[43] Complexes possessing Gd−O−Gd angles (θ) 109° > θ > 132° are found to be antiferromagnetic. Since the J_5 pathway involves Gd−O−Gd angles of 100.7° and 108.2°, this is expected to yield weak antiferromagnetic exchange as calculated with the broken-symmetry approach. Extremely small J values for the Gd···Gd pairs are associated with the inert nature of the 4f orbitals, and the mechanism of coupling is found to occur via the empty 5d/6s/6p orbitals of the Gd(III) ion.[43] The J_6 interaction is mediated via the μ_5-O group where the Gd−O−Gd angle is found to be 175°. Although the developed correlation is not applicable here as it is a singly bridged Gd···Gd interaction, at this near-linear Gd−O−Gd angle, the 4f orbitals of the Gd(III) ions will be either orthogonal or weakly interacting (see Supporting Information Table ST6, SF5), and this is expected to yield a weak ferromagnetic interaction. In complex **2**, the Gd···Gd J_5* interaction is in fact a next-nearest-neighbor interaction where the two Gd(III) centers are not directly connected to each other, and thus extremely weak coupling is expected.

Correlation to Experiment and Spin Density Analysis. The dominant Cu···Cu interaction estimated for complex **1** is J_1 which fixes the spin down on the central Cu(II) center and spin-up on the outer Cu(II) centers. The dominant Cu···Gd interaction is J_3 which is antiferromagnetic, leading to a spin-up configuration for the Gd(III) ions, thus yielding a $S = {}^{31}/_{2}$ ground state (see Figure 1b). The antiferromagnetic J_3 and J_5

DOI: 10.1021/ic502651w
Inorg. Chem. 2015, 54, 1661−1670

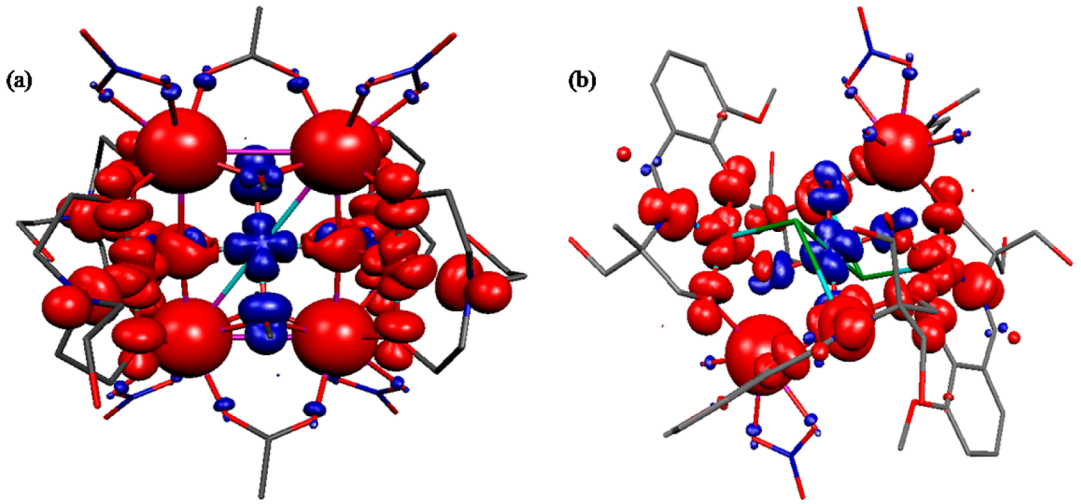

Figure 4. Spin density plot of (a) complex **1** for $S = {}^{31}/_{2}$ spin state and (b) complex **2** for $S = {}^{17}/_{2}$ spin state. The red and blue region represents positive and negative spin densities, respectively.

interactions are competing with each other, thus reducing the energy gap between ground and excited states.

The computed J values for complex **1** yield an $S = {}^{31}/_{2}$ ground state, contradictory to the original report of $S = {}^{23}/_{2}$.[62] Although the experimentally extracted J values are grossly different to those computed for complex **1**, they both fit the magnetic data reasonably well (see Figure 2a,b). The $S = {}^{23}/_{2}$ state predicted by the experiment fit is only 1.6 cm^{-1} in energy above the $S = {}^{31}/_{2}$ ground state when our DFT exchange values are employed. The small energy gap between these states and the large number of parameters required to fit the data (five exchange interactions and one g value) render the system overparameterized and thus explain such multiple local minima.

Intermolecular magnetic correlations, e.g., dipole−dipole coupling, further complicate the interpretation of the magnetic properties. Assuming each molecule as a point-like dipole with $S = {}^{31}/_{2}$, the maximum value of the dipolar interaction energy between nearest-neighboring molecules (far apart from each other by $r = 7.9$ Å, see Figure SF10 of Supporting Information) is $(g\mu_B S)^2/r^3 \approx 0.4$ cm^{-1}. While this value is an upper bound, one can reasonably expect the dipolar field to be of the order of ca. 0.02 T, which is characteristic for systems of dipolar coupled molecular nanomagnets.[74] The point is that the strength of such interactions is likely comparable to the very weak Cu−Gd and Gd−Gd intramolecular couplings in complex **1** (see J_3, J_4, and J_5 in Table 2). Unfortunately, dipolar interactions are impossible to fully implement in DFT calculations, thus limiting our simulations to the modeling of the magnetic properties of noninteracting, individual molecules. Nevertheless, we can arguably deduce the following, important information by comparing the so-obtained DFT simulations with the experimental data. Note that the experimental susceptibility lies below the calculated curve for noninteracting molecules at low temperatures (see Figure 2a), and the experimental magnetization behaves likewise with respect to the corresponding simlulations at low fields and temperatures (Figure 2b). The only plausible explanation is that each molecule in complex **1** carries a lower net spin state, viz., the intermolecular interactions narrow the gap between the $S = {}^{31}/_{2}$ ground state (as expected in the absence of such interactions) and the low-lying excited states, which are characterized by lower spin values. As an illustrative example, we have mimicked the effect of intermolecular interactions by computing the magnetothermal properties of a simplified model system, thus different than **1**, consisting of two molecules magnetically correlated by weak J coupling constants of the order of 10^{-2} cm^{-1} (see Supporting Information, specifically SF12, SD4, and SF13, for details).

The computed spin density plot of the $S = {}^{31}/_{2}$ ground state is shown in Figure 4a. All the Gd(III) ions have spin density ∼7.01, while the central Cu(II) ions has slightly higher spin density than the terminal Cu(II) centers (−0.65 vs 0.62). To further elucidate the electronic differences, spin densities in a $\{Cu_3Gd_2\}$ unit (a part of full structure, **1**) will be considered from the $S = {}^{31}/_{2}$ ground state solution. The central μ_5-O group in $\{Cu_3Gd_2\}$ (see Figure SF6a, Supporting Information) of **1** is found to have a spin density of 0.27 and a major part of this density is likely to be gained from the Cu(II) via spin delocalization since all the three Cu(II) $d_{x^2-y^2}$ orbitals are directed toward this atom.

For complex **2**, both the susceptibility and the magnetization data are very well reproduced by the DFT computed J values (see Figure 2b,c).[75] The parameters obtained yielded an $S = {}^{17}/_{2}$ ground state, in agreement with the experiment. Similarly to **1**, this ground state for complex **2** has the central Cu(II) ion spin-down, while the other Cu(II) centers are spin-up due to dominant J_1 interactions. Both the Cu···Gd interactions (J_3 and J_4) are computed to be ferromagnetic, but J_3 is stronger than J_4, resulting in a spin-up orientation of the Gd(III) centers. The ground state spin density plot for $S = {}^{17}/_{2}$ is shown in Figure 4b. The central μ_3-O atoms of the $\{Cu_2Gd\}$ core (see Figure SF6b, Supporting Information) are found to possess significant spin density compared to other atoms (0.12, 0.14), but the magnitude is significantly smaller than that of complex **1** ($\{Cu_2Gd\}$ unit is a part of full structure **2**, as considered from the $S = {}^{17}/_{2}$ ground state solution).

Effect of Exchange Interaction in the Estimation of MCE Values. The maximum possible $-\Delta S_m$ value are set by the entropy content of the corresponding uncoupled single-ion spins s_i, i.e., $\sum_i R \ln(2s_i + 1)$, which provides 45.8 and 34.9 J kg^{-1} K^{-1} for complexes **1** and **2**, respectively. Experimental $-\Delta S_m$ values are smaller than these maxima due to the presence of nonzero exchange interactions. From magnetization (M) data, the ΔS_m can be estimated using the Maxwell

DOI: 10.1021/ic502651w
Inorg. Chem. 2015, 54, 1661−1670

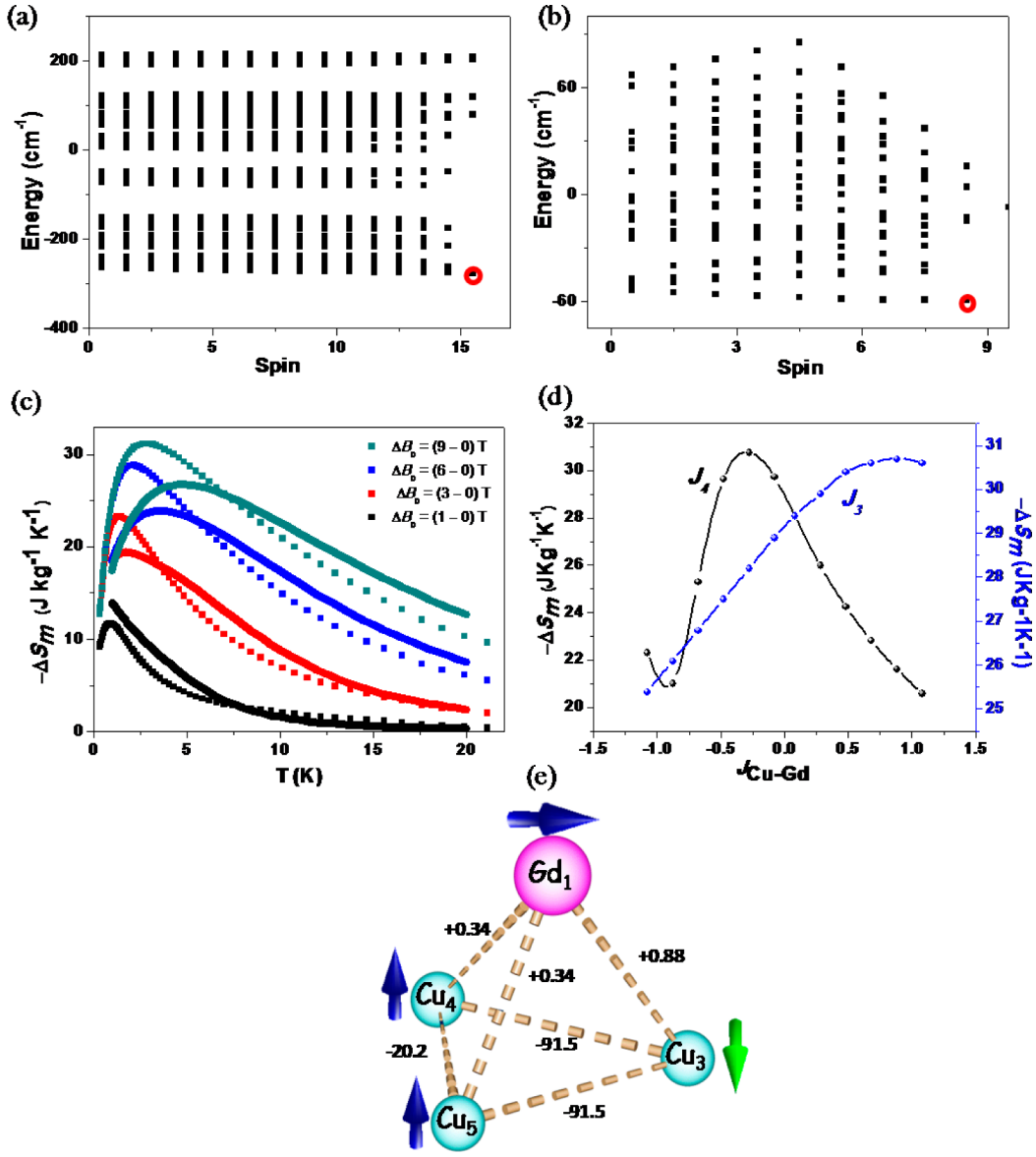

Figure 5. (a) Eigenvalue plot of complex **1** using the DFT derived exchange parameters, showing only the excited states close to ground state (the ground state highlighted with a red circle, see Figure SF10 (a) for complete Eigen plot); (b) eigenvalue plot of complex **2** using the DFT derived exchange parameters, showing only the excited states close to ground state (the ground state is highlighted with a red circle, see Figure SF10 (b) for complete Eigen plot); (c) simulated ΔS_M versus T curves using DFT J values (solid lines) and experimental points (filled circles); (d) correlation developed by varying J_3 and J_4 values in complex **1**; (e) a representative $\{Cu_3Gd\}$ unit designed out of complex **1** (Figure 1b); labels are essentially same as in Figure 1b.

relation[10] $\Delta S_m(T)\Delta_B = \int [((\partial M(T,B))/(\partial T))]_B \, dB$. The computed $-\Delta S_m$ versus T plot for complex **1** (see Supporting Information, Figure SF7 for complex **2**) simulated using DFT calculated J values is shown in Figure 5c. It is worth pointing out that, because of the derivative in the Maxwell relation, ΔS_m is extremely sensitive to the field and temperature dependencies of the magnetization data. Therefore, the relatively good agreement between simulated and experimental M data for complex **1** (Figure 2b) is somewhat less satisfactory in the case of the simulated and experimental entropy changes in Figure 5c. The maximum $-S_m$, as obtained from specific heat experiments,[12] is ∼31 J kg^{-1} K^{-1} (3 K and ΔB = 9 T), whereas that calculated with the DFT exchange parameters is 25.4 J kg^{-1} K^{-1} at 3 K and ΔB = 9 T. For complex **1**, the relatively higher experimental values of $-\Delta S_m$, i.e., the stronger field dependence of the MCE at low temperatures, imply a larger number of spin states that become available at such temperatures.[76] As also illustrated by the simplified model system in Supporting Information (see Figure SF13), this implication can be understood by the aforementioned observation that excited spin states are lying closer to the ground state because of intermolecular interactions, which are not specifically considered in our simulations for complex **1**. For complex **2**, the calculated $-\Delta S_m$ value is 19.3 J kg^{-1} K^{-1} at 3 K and ΔB = 9 T (see Figure SF7 of Supporting Information); however, experimental data are not available for this complex.

Clearly, the large value of $-\Delta S_m$ observed for complex **1** is due to very weak Cu···Gd and Gd···Gd interactions which leads to small gaps between the ground and lowest excited states, Figure 5a. The strong antiferromagnetic J_1 interaction is responsible for the relatively large gaps in the spectrum (see Figure SF11). If J_1 and J_2 were weak, then the states would

DOI: 10.1021/ic502651w
Inorg. Chem. 2015, 54, 1661−1670

resemble a continuum leading to even larger $-\Delta S_m$ values. Nevertheless, J_1 and J_2 are competing with each other, thus helping in reducing the gap and enhancing $-\Delta S_m$. Taken individually, both the J_1 and J_2 interactions are extremely strong, and therefore small variations to these J values have negligible effect on the $-\Delta S_m$ values, Table ST15, Supporting Information. This is quite understandable given the fact that the quoted $-\Delta S_m$ values are obtained at 3 K and at 9 T applied field where the thermal energy window is about 2 cm^{-1}. Unless the J_1 and J_2 interactions are significantly weaker (say less than 10 cm^{-1}, see Table ST15 of Supporting Information), its contribution to the $-\Delta S_m$ is negligible. Small J_1 and J_2 parameters are obtained when the Cu−O−Cu angles are in the range of 92−95 deg, as shown in Figure 2e, and although this parameter is difficult to vary within a cluster, deliberate structural distortion in a family of $\{Mn^{III}_6\}$ clusters was achieved,[77] suggesting that this approach is not impossible. Another route to such a modification is through the application of pressure to alter the bond angles;[78,79] however, this has not been attempted in large clusters such as these.

For both the complexes, the Cu···Gd J_3 and J_4 interactions yield mixed, weak ferro/antiferromagnetic behavior. Since this interaction is tunable as illustrated in the correlation above and the exchange values lie within the energy window of 2 cm^{-1} (see Table 2), we have developed a magnetic-entropy vs magnetic exchange correlations (exchange-entropy correlations) for Cu···Gd interactions present in complex **1** to understand the impact of these J values on $-\Delta S_m$ (see Figure 5d). Here the $-\Delta S_m$ is estimated by varying J_3 and J_4 interactions (independently) while keeping the other exchange values constant. An increase in $-\Delta S_m$ with an increase in J_3 was observed with the largest achievable $-\Delta S_m$ value of 30.7 J kg^{-1} K^{-1} was observed at J_3 = +0.88 cm^{-1} (increase of about 5.3 J kg^{-1} K^{-1} for change in the exchange values within 1 cm^{-1}), corresponding to spin frustration within the $\{Cu_3Gd\}$ units of complex **1** (see Figure 5e for a representative $\{Cu_3Gd\}$ unit). Although the magnitude of the $-\Delta S_m$values are found to be strongly correlated to other exchange interactions as well (see Supporting Information, Figure SF9), the large increases are due to the collapsing of the excited spin states toward the ground state. Within 2 cm^{-1} of the ground state ∼60 states exist when J_3 = +0.88 cm^{-1} compared to just six states when J_3 = −1.08 cm^{-1}. For J_4, a Gaussian type curve was noted with a peak at $J_4 \approx -0.28$ cm^{-1}, again corresponding to a frustrated situation.

Another approach to enhance the MCE is to increase the number of unpaired electrons within the system. We have computed the J_1 interaction on model complexes (see Figure SF2a, Supporting Information for structure of model dimer) where we have substituted the Cu(II) sites for Fe(II), Mn(II), and Ni(II). The estimated J_1 parameters for these fictitious models are −10.90 cm^{-1}, −17.15 cm^{-1}, and −14.99 cm^{-1} respectively. Although both Fe(II) and Ni(II) ions offer weaker exchange interactions compared to Cu(II), they are also likely to possess significant magnetic anisotropy which could be detrimental to the MCE. The best candidate is therefore Mn(II) where the magnetic anisotropy is likely to be negligible and would lead to higher degeneracy due to a larger spin.

Finally, our simulations indirectly reveal the profound influence that intermolecular correlations might represent for the MCE in this type of magnetic molecules. For complex **1**, a weak yet noticeable intermolecular interaction (e.g., dipolar coupling) is sufficient for considerably increasing the field dependence of $-\Delta S_m$ at low temperatures. This suggests that the dipolar coupling is yet another ingredient to be considered for making an optimized magnetic refrigerant for such low temperatures.[1] Tentatively, one could play with the crystallographic packing of the molecules as such to change the dipolar field, as, e.g., successfully accomplished for the $\{Fe_{17}\}$ molecular nanomagnet.[80] Note that, for antiferromagnetic molecules, the field dependence of the MCE can be increased for values of the (dipolar) field that specifically depends on the spin levels structure.[81] As an unavoidable side effect, it should also be mentioned that the dipolar field will ultimately limit the lowest temperature, attainable by adiabatic refrigeration.[82]

CONCLUSIONS

Two structurally similar polynuclear $\{Cu_5Gd_n\}$ (where n = 4, 2) clusters were modeled using DFT methods to elucidate the nature of the magnetic exchange pathways in these clusters and to probe the origin of large MCE. A large discrepancy between the previously extracted exchange parameters obtained by fitting the magnetic data, and the computed parameter values are noted and this is due to an overparameterization of the problem. Invariably, this analysis suggests that the magnetic interactions within such large heterogeneous clusters cannot be reliably modeled without input from computational methods. If such calculations are not viable, existing magnetostructural correlations describing appropriate exchange pairs should be used to obtain qualitative estimates of coupling parameters which then can be refined by fitting the magnetic data. This is particularly important for 3d-Gd clusters as the magnetic exchange in such clusters decreases by an order of magnitude as we go from 3d-3d (∼ in the range of 10^3 to 10 cm^{-1})[66,68,53] to 3d-Gd (∼ in the range of 10 to 0.1 cm^{-1})[83−86] and Gd−Gd interactions (∼ in the range of 10^{-3} to 0.1 cm^{-1}).[25−31] In many instances these extremely weak 3d-Gd and Gd−Gd interactions are masked by the strong 3d-3d interactions resulting in a likely overparameterization problem even in smaller clusters.

The ground state of **1** as estimated by experiments of $S = {}^{23}/_2$ and $S = {}^{17}/_2$ is found to be erroneous, and we suggest that $S = {}^{31}/_2$ is more likey the true ground state. Since some of the interactions are extremely weak, close to 100 states are found within 10 cm^{-1} of the ground state for complex **1**. This makes the interpretation of the magnetic data extremely challenging and hence explains the discrepancy between the present interpretation and the original analysis.[62] This misinterpretation due to overparameterization has been remedied here by DFT calculations. The ground state of **2** as elucided experimentally was found to be in agreement with the computed results, of $S = {}^{17}/_2$, despite some inconsistencies with the original and calculated exchange values, which is also a result of overparameterization.

A two-dimensional magnetostructural correlation for the $\{Cu(OR)_2Gd\}$ pair has been developed to rationalize the observed Cu···Gd interactions within these complexes. Our results demonstrate the pivotal role of the Cu−O−Gd angle in controlling the sign of the magnetic exchange. Although acute Cu−O−Gd angles are not often found on dimeric structures, tight angles are often observed in polynuclear complexes and may hold the key in determining the sign as well as the strength of the exchange interactions.

The large MCE in complex **1** is found to be associated with the very small Cu···Gd and Gd···Gd interactions, and the strongly antiferromagnetic Cu···Cu interactions are found to be

DOI: 10.1021/ic502651w
Inorg. Chem. 2015, 54, 1661−1670

detrimental to the $-\Delta S_m$ values. The exchange-entropy correlations suggest that modulating J values to achieve spin frustration is a viable way to enhance the MCE values. Controlling structural parameters such as the Cu−O−Cu and Cu−O−Gd angles or substituting the Cu(II) ions for Mn(II) is predicted to enhance the MCE.

■ ASSOCIATED CONTENT

Supporting Information

Information such as spin density plots, overlap integral values, selected structural parameters corresponding to each J values, dinuclear models for each J values, simulated magnetic susceptibility vs temperature data of **2** etc. This material is available free of charge via the Internet at http://pubs.acs.org.

■ AUTHOR INFORMATION

Corresponding Author

*Fax: (+91)-22-2576-7152. Tel: (+91)-22-2576-7183. E-mail: rajaraman@chem.iitb.ac.in.

Notes

The authors declare no competing financial interest.

■ ACKNOWLEDGMENTS

G.R. would like to acknowledge financial support from DST India (SR/S1/IC-41/2010; SR/NM/NS-1119/2011) and IIT Bombay for access to the high performance computing facility. T.R. acknowldges a SRF position from DST, India. G.R. and K.S.M. acknowledge the support of an Australia-India Strategic Research grant (DST/INT/AUS/P-47/11). M.E. acknowledges financial support from the Spanish MINECO (MAT2012-38318-C03-01). N.F.C. thanks The University of Manchester for a President's Doctoral Scholarship.

■ REFERENCES

(1) Evangelisti, M.; Brechin, E. K. *Dalton Trans.* **2010**, *39*, 4672−4676.
(2) Weiss, P.; Piccard, A. *J. Phys. (Paris)* **1917**, 5th Ser. 7, 103−109.
(3) Debye, P. *Ann. Phys.* **1926**, *81*, 1154−1160.
(4) Giauque, W. F. *J. Am. Chem. Soc.* **1927**, *49*, 1864−1870.
(5) Feder, T. *Phys. Today* **2009**, *62*, 21−23.
(6) Shaw, R.; Laye, R. H.; Jones, L. F.; Low, D. M.; Talbot-Eeckelaers, C.; Wei, Q.; Milios, C. J.; Teat, S.; Helliwell, M.; Raftery, J.; Evangelisti, M.; Affronte, M.; Collison, D.; Brechin, E. K.; McInnes, E. J. L. *Inorg. Chem.* **2007**, *46*, 4968−4978.
(7) Evangelisti, M.; Luis, F.; de Jongh, L. J.; Affronte, M. *J. Mater. Chem.* **2006**, *16*, 2534−2549.
(8) Gatteschi, D.; Sessoli, R.; Villain, J. *Molecular Nanomagnets*; OUP: Oxford, 2006; pp 1−10.
(9) Torres, F.; Hernandez, J. M.; Bohigas, X.; Tejada, J. *Appl. Phys. Lett.* **2000**, *77*, 3248−3250.
(10) Evangelisti, M.; Candini, A.; Ghirri, A.; Affronte, M.; Brechin, E. K.; McInnes, E. J. L. *Appl. Phys. Lett.* **2005**, *87*, 072504:1−072504:3.
(11) Cremades, E.; Gomez-Coca, S.; Aravena, D.; Alvarez, S.; Ruiz, E. *J. Am. Chem. Soc.* **2012**, *134*, 10532−10542.
(12) Langley, S. K.; Chilton, N. F.; Moubaraki, B.; Hooper, T.; Brechin, E. K.; Evangelisti, M.; Murray, K. S. *Chem. Sci.* **2011**, *2*, 1166−1169.
(13) Zheng, Y. Z.; Evangelisti, M.; Winpenny, R. E. P. *Chem. Sci.* **2011**, *2*, 99−102.
(14) Zheng, Y. Z.; Evangelisti, M.; Winpenny, R. E. P. *Angew. Chem., Int. Ed. Engl.* **2011**, *50*, 3692−3695.
(15) Karotsis, G.; Evangelisti, M.; Dalgarno, S. J.; Brechin, E. K. *Angew. Chem., Int. Ed. Engl.* **2009**, *48*, 9928−9931.
(16) Peng, J. B.; Zhang, Q. C.; Kong, X. J.; Zheng, Y. Z.; Ren, Y. P.; Long, L. S.; Huang, R. B.; Zheng, L. S.; Zheng, Z. P. *J. Am. Chem. Soc.* **2012**, *134*, 3314−3317.
(17) Guo, F. S.; Chen, Y. C.; Liu, J. L.; Leng, J. D.; Meng, Z. S.; Vrabel, P.; Orendac, M.; Tong, M. L. *Chem. Commun.* **2012**, *48*, 12219−12221.
(18) Dermitzaki, D.; Lorusso, G.; Raptopoulou, C. P.; Psycharis, V.; Escuer, A.; Evangelisti, M.; Perlepes, S. P.; Stamatatos, T. C. *Inorg. Chem.* **2013**, *52*, 10235−10237.
(19) Hooper, T. N.; Inglis, R.; Palacios, M. A.; Nichol, G. S.; Pitak, M. B.; Coles, S. J.; Lorusso, G.; Evangelisti, M.; Brechin, E. K. *Chem. Commun.* **2014**, *50*, 3498−3500.
(20) Peng, J. B.; Zhang, Q. C.; Kong, X. J.; Ren, Y. P.; Long, L. S.; Huang, R. B.; Zheng, L. S.; Zheng, Z. *Angew. Chem.Int. Ed.* **2011**, *50*, 10649−10652.
(21) Zheng, Y.-Z.; Pineda, E. M.; Helliwell, M.; Winpenny, R. E. P. *Chem.—Eur. J.* **2012**, *18*, 4161−4165.
(22) Pineda, E. M.; Tuna, F.; Pritchard, R. G.; Regan, A. C.; Winpenny, R. E. P.; McInnes, E. J. L. *Chem. Commun.* **2013**, *49*, 3522−3524.
(23) Birk, T.; Pedersen, K. S.; Thuesen, C. A.; Weyhermuller, T.; Schau-Magnussen, M.; Piligkos, S.; Weihe, H.; Mossin, S.; Evangelisti, M.; Bendix, J. *Inorg. Chem.* **2012**, *51*, 5435−5443.
(24) Zheng, Y.-Z.; Evangelisti, M.; Tuna, F.; Winpenny, R. E. P. *J. Am. Chem. Soc.* **2012**, *134*, 1057−1065.
(25) Zhang, Z.-M.; Pan, L.-Y.; Lin, W.-Q.; Leng, J.-D.; Guo, F.-S.; Chen, Y.-C.; Liu, J.-L.; Tong, M.-L. *Chem. Commun.* **2013**, *49*, 8081−8083.
(26) Evangelisti, M.; Roubeau, O.; Palacios, E.; Camon, A.; Hooper, T. N.; Brechin, E. K.; Alonso, J. J. *Angew. Chem., Int. Ed. Engl.* **2011**, *50*, 6606−6609.
(27) Guo, F. S.; Leng, J. D.; Liu, J. L.; Meng, Z. S.; Tong, M. L. *Inorg. Chem.* **2012**, *51*, 405−413.
(28) Sharples, J. W.; Zheng, Y. Z.; Tuna, F.; McInnes, E. J. L.; Collison, D. *Chem. Commun.* **2011**, *47*, 7650−7652.
(29) Chang, L. X.; Xiong, G.; Wang, L.; Cheng, P.; Zhao, B. *Chem. Commun.* **2013**, *49*, 1055−1057.
(30) Hooper, T. N.; Schnack, J.; Piligkos, S.; Evangelisti, M.; Brechin, E. K. *Angew. Chem., Int. Ed. Engl.* **2012**, *51*, 4633−4636.
(31) Jia, J.-M.; Liu, S.-J.; Cui, Y.; Han, S.-D.; Hu, T.-L.; Bu, X.-H. *Cryst. Growth Des* **2013**, *13*, 4631−4634.
(32) Chen, Y.-C.; Guo, F.-S.; Liu, J.-L.; Leng, J.-D.; Vrábel, P.; Orendáč, M.; Prokleška, J.; Sechovský, V.; Tong, M.-L. *Chem.—Eur. J.* **2014**, *20*, 3029−3035.
(33) Lorusso, G.; Jenkins, M.; Gonzalez-Monje, P.; Arauzo, A.; Sese, J.; Ruiz-Molina, D.; Roubeau, O.; Evangelisti, M. *Adv. Mater.* **2013**, *25*, 2984−2988.
(34) Liu, J. L.; Chen, Y. C.; Li, Q. W.; Gomez-Coca, S.; Aravena, D.; Ruiz, E.; Lin, W. Q.; Leng, J. D.; Tong, M. L. *Chem. Commun.* **2013**, *49*, 6549−6551.
(35) Milios, C. J.; Manoli, M.; Rajaraman, G.; Mishra, A.; Budd, L. E.; White, F.; Parsons, S.; Wernsdorfer, W.; Christou, G.; Brechin, E. K. *Inorg. Chem.* **2006**, *45*, 6782−6793.
(36) Rajaraman, G.; Cano, J.; Brechin, E. K.; McInnes, E. J. L. *Chem. Commun.* **2004**, 1476−1477.
(37) Rajaraman, G.; Ruiz, E.; Cano, J.; Alvarez, S. *Chem. Phys. Lett.* **2005**, *415*, 6−9.
(38) Rajeshkumar, T.; Rajaraman, G. *Chem. Commun.* **2012**, *48*, 7856−7858.
(39) Singh, S. K.; Pedersen, K. S.; Sigrist, M.; Thuesen, C. A.; Schau-Magnussen, M.; Mutka, H.; Piligkos, S.; Weihe, H.; Rajaraman, G.; Bendix, J. *Chem. Commun.* **2013**, *49*, 5583−5585.
(40) Singh, S. K.; Rajaraman, G. *Dalton Trans.* **2013**, *42*, 3623−3630.
(41) Singh, S. K.; Tibrewal, N. K.; Rajaraman, G. *Dalton Trans.* **2011**, *40*, 10897−10906.
(42) Baker, M. L.; Timco, G. A.; Piligkos, S.; Mathieson, J. S.; Mutka, H.; Tuna, F.; Kozlowski, P.; Antkowiak, M.; Guidi, T.; Gupta, T.; Rath, H.; Woolfson, R. J.; Kamieniarz, G.; Pritchard, R. G.; Weihe, H.;

DOI: 10.1021/ic502651w
Inorg. Chem. 2015, 54, 1661−1670

Cronin, L.; Rajaraman, G.; Collison, D.; McInnes, E. J. L.; Winpenny, R. E. P. *Proc. Natl. Acad. Sci. U. S. A.* **2012**, *109*, 19113−19118.
(43) Rajeshkumar, T.; Singh, S. K.; Rajaraman, G. *Polyhedron* **2013**, *52*, 1299−1305.
(44) Liu, J. L.; Lin, W. Q.; Chen, Y. C.; Gomez-Coca, S.; Aravena, D.; Ruiz, E.; Leng, J. D.; Tong, M. L. *Chem.—Eur. J.* **2013**, *19*, 17567−17577.
(45) Anwar, M. U.; Dawe, L. N.; Tandon, S. S.; Bunge, S. D.; Thompson, L. K. *Dalton Trans.* **2013**, *42*, 7781−7794.
(46) Canadillas-Delgado, L.; Fabelo, O.; Pasan, J.; Delgado, F. S.; Lloret, F.; Julve, M.; Ruiz-Perez, C. *Dalton Trans.* **2010**, *39*, 7286−7293.
(47) Leng, J. D.; Liu, J. L.; Tong, M. L. *Chem. Commun.* **2012**, *48*, 5286−5288.
(48) Dinca, A. S.; Ghirri, A.; Madalan, A. M.; Affronte, M.; Andruh, M. *Inorg. Chem.* **2012**, *51*, 3935−3937.
(49) Wu, G.; Hewitt, I. J.; Mameri, S.; Lan, Y.; Clerac, R.; Anson, C. E.; Qiu, S.; Powell, A. K. *Inorg. Chem.* **2007**, *46*, 7229−7231.
(50) Bencini, A.; Totti, F. *Int. J. Quantum Chem.* **2005**, *101*, 819−825.
(51) Noodleman, L. *J. Chem. Phys.* **1981**, *74*, 5737−5743.
(52) Christian, P.; Rajaraman, G.; Harrison, A.; McDouall, J. J. W.; Raftery, J. T.; Winpenny, R. E. P. *Dalton Trans.* **2004**, 1511−1512.
(53) Ruiz, E.; Alvarez, S.; Rodriguez-Fortea, A.; Alemany, P.; Pouillon, Y.; Massobrio, C. In *Magnetism: Molecules to Materials II*; Miller, J. S., Drillon, M., Eds.; Wiley-VCH: Weinheim, 2001; p 227−280.
(54) Rajaraman, G.; Totti, F.; Bencini, A.; Caneschi, A.; Sessoli, R.; Gatteschi, D. *Dalton Trans.* **2009**, 3153−3161.
(55) Becke, A. D. *J. Chem. Phys.* **1993**, *98*, 5648−5652.
(56) Schafer, A.; Huber, C.; Ahlrichs, R. *J. Chem. Phys.* **1994**, *100*, 5829−5835.
(57) Cundari, T. R.; Stevens, W. J. *J. Chem. Phys.* **1993**, *98*, 5555−5565.
(58) Frisch, M. J.; Trucks, G. W.; Schlegel, H. B.; Scuseria, G. E.; Robb, M. A.; Cheeseman, J. R.; Scalmani, G.; Barone, V.; Mennucci, B.; Petersson, G. A.; Nakatsuji, H.; Caricato, M.; Li, X.; Hratchian, H. P.; Izmaylov, A. F.; Bloino, J.; Zheng, G.; Sonnenberg, J. L.; Hada, M.; Ehara, M.; Toyota, K.; Fukuda, R.; Hasegawa, J.; Ishida, M.; Nakajima, T.; Honda, Y.; Kitao, O.; Nakai, H.; Vreven, T.; Montgomery, J. A., Jr.; Peralta, J. E.; Ogliaro, F.; Bearpark, M.; Heyd, J. J.; Brothers, E.; Kudin, K. N.; Staroverov, V. N.; Kobayashi, R.; Normand, J.; Raghavachari, K.; Rendell, A.; Burant, J. C.; Iyengar, S. S.; Tomasi, J.; Cossi, M.; Rega, N.; Millam, N. J.; Klene, M.; Knox, J. E.; Cross, J. B.; Bakken, V.; Adamo, C.; Jaramillo, J.; Gomperts, R.; Stratmann, R. E.; Yazyev, O.; Austin, A. J.; Cammi, R.; Pomelli, C.; Ochterski, J. W.; Martin, R. L.; Morokuma, K.; Zakrzewski, V. G.; Voth, G. A.; Salvador, P.; Dannenberg, J. J.; Dapprich, S.; Daniels, A. D.; Farkas, Ö.; Foresman, J. B.; Ortiz, J. V.; Cioslowski, J.; Fox, D. J. *Gaussian 09*, Revision A.02; Gaussian, Inc.: Wallingford, CT, 2009.
(59) Borras-Almenar, J. J.; Clemente-Juan, J. M.; Coronado, E.; Tsukerblat, B. S. *J. Comput. Chem.* **2001**, *22*, 985−991.
(60) Chilton, N. F.; Anderson, R. P.; Turner, L. D.; Soncini, A.; Murray, K. S. *J. Comput. Chem.* **2013**, *34*, 1164−1175.
(61) Sessoli, R. *Angew. Chem., Int. Ed. Engl.* **2012**, *51*, 43−45.
(62) Langley, S. K.; Ungur, L.; Chilton, N. F.; Moubaraki, B.; Chibotaru, L. F.; Murray, K. S. *Chem.—Eur. J.* **2011**, *17*, 9209−9218.
(63) Ruiz, E.; Cano, J.; Alvarez, S.; Caneschi, A.; Gatteschi, D. *J. Am. Chem. Soc.* **2003**, *125*, 6791−6794.
(64) Kahn, O. *Molecular Magnetism*; VCH: Weinheim, 1993; pp 145−183.
(65) Crawford, V. H.; Richardson, H. W.; Wasson, J. R.; Hodgson, D. J.; Hatfield, W. E. *Inorg. Chem.* **1976**, *15*, 2107−2110.
(66) Ruiz, E.; Alemany, P.; Alvarez, S.; Cano, J. *J. Am. Chem. Soc.* **1997**, *119*, 1297−1303.
(67) Haddad, M. S.; Wilson, S. R.; Hodgson, D. J.; Hendrickson, D. N. *J. Am. Chem. Soc.* **1981**, *103*, 384−391.
(68) Ruiz, E.; Alemany, P.; Alvarez, S.; Cano, J. *Inorg. Chem.* **1997**, *36*, 3683−3688.
(69) Angaroni, M.; Ardizzoia, G. A.; Beringhelli, T.; Lamonica, G.; Gatteschi, D.; Masciocchi, N.; Moret, M. *J. Chem. Soc., Dalton Trans.* **1990**, 3305−3309.
(70) Butcher, R. J.; Oconnor, C. J.; Sinn, E. *Inorg. Chem.* **1981**, *20*, 537−545.
(71) Ferrer, S.; Haasnoot, J. G.; Reedijk, J.; Muller, E.; Cingi, M. B.; Lanfranchi, M.; Lanfredi, A. M. M.; Ribas, J. *Inorg. Chem.* **2000**, *39*, 1859−1867.
(72) Rodriguez-Fortea, A.; Alemany, P.; Alvarez, S.; Ruiz, E. *Inorg. Chem.* **2002**, *41*, 3769−3778.
(73) Cirera, J.; Ruiz, E. *C. R. Chim.* **2008**, *11*, 1227−1234.
(74) Luis, F. Dipolar magnetic order in crystals of molecular nanomagnets. In *Molecular Magnets, NanoScience and Technology*; Bartolomé, J., Luis, F., Fernández, J. F., Eds.; Springer-Verlag: Berlin, 2014; pp 161−190.
(75) Note: The experimental points here are extracted using GetData Graph Digitizer software.
(76) Evangelisti, M.; Candini, A.; Affronte, M.; Pasca, E.; de Jongh, L. J.; Scott, R. T. W.; Brechin, E. K. *Phys. Rev. B* **2009**, *79*, 104414:1−104414:5.
(77) Inglis, R.; Jones, L. F.; Milios, C. J.; Datta, S.; Collins, A.; Parsons, S.; Wernsdorfer, W.; Hill, S.; Perlepes, S. P.; Piligkos, S.; Brechin, E. K. *Dalton Trans.* **2009**, 3403−3412.
(78) Parois, P.; Moggach, S. A.; Sanchez-Benitez, J.; Kamenev, K. V.; Lennie, A. R.; Warren, J. E.; Brechin, E. K.; Parsons, S.; Murrie, M. *Chem. Commun.* **2010**, *46*, 1881−1883.
(79) Prescimone, A.; Sanchez-Benitez, J.; Kamenev, K. K.; Moggach, S. A.; Warren, J. E.; Lennie, A. R.; Murrie, M.; Parsons, S.; Brechin, E. K. *Dalton Trans.* **2010**, *39*, 113−123.
(80) (a) Evangelisti, M.; Candini, A.; Ghirri, A.; Affronte, M.; Powell, G. W.; Gass, I. A.; Wood, P. A.; Parsons, S.; Brechin, E. K.; Collison, D.; Heath, S. L. *Phys. Rev. Lett.* **2006**, *97*, 167202:1−167202:4. (b) Gass, I. A.; Brechin, E. K.; Evangelisti, M. *Polyhedron* **2013**, *52*, 1177−1180.
(81) Sharples, J. W.; Collison, D.; McInnes, E. J. L.; Schnack, J.; Palacios, E.; Evangelisti, M. *Nat. Commun.* **2014**, *5*, 5321:1−5321:5.
(82) Martínez-Pérez, M. J.; Montero, O.; Evangelisti, M.; Luis, F.; Sesé, J.; Cardona-Serra, S.; Coronado, E. *Adv. Mater.* **2012**, *24*, 4301−4305.
(83) Costes, J.-P.; Dahan, F.; Donnadieu, B.; Fernadez-Garcia, M. I.; Rodriguez-Douton, M. J. *Dalton Trans.* **2003**, 3776−3779.
(84) Costes, J.-P.; Dahan, F.; Garcia-Tojal, J. *Chem.—Eur. J.* **2002**, *8*, 5430−5434.
(85) Costes, J.-P.; Dahan, F.; Dupuis, A.; Laurent, J. P. *Inorg. Chem.* **1997**, *36*, 4284−4286.
(86) Costes, J.-P.; Yamaguchi, T.; Kojima, M.; Vendier, L. *Inorg. Chem.* **2009**, *48*, 5555−5561.

DOI: 10.1021/ic502651w
Inorg. Chem. 2015, 54, 1661−1670